

## Investigation of the Observed Edge Toroidal Rotation Acceleration Induced by Resonant Magnetic Perturbations in MAST-U

E.Tomasina<sup>1,2</sup>, T.Tala<sup>3</sup>, A.Salmi<sup>3</sup>, C.Albert<sup>4</sup>, J.Ball<sup>5</sup>, C.Beckley<sup>6</sup>, S.Blackmore<sup>6</sup>, L.Frassinetti<sup>7</sup>, G.S.Graßler<sup>4</sup>, A.Kirjasuo<sup>3</sup>, Y.Q.Liu<sup>8</sup>, C.Michael<sup>6</sup>, B.Patel<sup>6</sup>, L.Pigatto<sup>2</sup>, M.Poradzinski<sup>6</sup>, D.Ryan<sup>6</sup>, H.Sun<sup>5</sup>, T.Bolzonella<sup>2</sup>, MAST-U team<sup>\*</sup>, EUROfusion Tokamak Exploitation team<sup>\*\*</sup>

<sup>1</sup>Consorzio RFX (CNR, ENEA, INFN, University of Padova, Acciaierie Venete SpA), C.so Stati Uniti 4, 35127 Padova, Italy<sup>2</sup>CRF - University of Padova, Italy<sup>3</sup>Association EURATOM-Tekes, VTT, PO Box 1000, FIN-02044 VTT, Finland.<sup>4</sup>Fusion@OEAW, Graz, University of Technology, Graz, Austria<sup>5</sup>Ecole Polytechnique Fédérale de Lausanne (EPFL), Swiss Plasma Center (SPC), CH-1015 Lausanne, Switzerland.<sup>6</sup>UKAEA, Culham Campus, Abingdon OX14, 3DB, UK.<sup>7</sup>Division of Fusion Plasma Physics, KTH Royal Institute of Technology, Stockholm SE-100 44, Sweden.<sup>8</sup>General Atomics, PO Box 85608, San Diego, CA 92186-5608, USA. <sup>\*</sup>See author list of J.Harrison et al 2019 Nucl Fusion 59 112011. <sup>\*\*</sup>See the author list of E.Joffrin et al

2024 Nucl Fusion 64 112019

Given the foreseen absence of large momentum input (i.e. NBIs) in future reactor-scale devices and the importance of plasma rotation for MHD stability, identifying alternative actuators for rotation control is crucial. Evidence of rotation acceleration from controlled, external actions should thus be investigated. Resonant Magnetic Perturbations (RMPs) have drawn interest as potential momentum sources. In devices like TEXTOR, DIII-D, and EAST, plasma acceleration has been observed following the activation of external magnetic perturbations. TEXTOR's dynamic ergodic divertor (DED) produced non-axisymmetric perturbations resonant at the  $q = 3$  surface, forming a stochastic magnetic sea and inducing co- $I_p$  acceleration[1]. These results supported the theory of 'ergodic' torque from ion and electron motion in braided fields[2]. DIII-D and EAST observed plasma acceleration linked to non-resonant magnetic components, attributed to the Neoclassical Toroidal Viscous (NTV) torque. DIII-D observed counter- $I_p$  acceleration[3], whereas in EAST a co- $I_p$  flow was accelerated[4]. Both results can be explained using the standard NTV model, which associates counter- $I_p$ /co- $I_p$  torques to the ion and electron roots respectively[5]. Here, we report experimental and numerical evidence of a co- $I_p$  edge-localized torque during MAST-U discharges, unlike previous MAST experiments, which showed no such effect[6].

### Experiments Setup

The MAST-U non-axisymmetric coil system comprises an in-vessel set of 'ELM' coils, four in the upper row and eight in the lower, as well as a set of four larger ex-vessel coils dedicated to Error Field Correction (EFCCs). Recently, two experimental campaigns were conducted to investigate momentum transport induced by RMPs, utilizing only the in-vessel coils. In the first campaign, the ELM coil system operated in an  $n = 4$  configuration (with  $n$  being the toroidal mode number), thus employing only the lower row of coils. The discharges were L-mode Connected Double Null (CDN) configurations with a toroidal magnetic field  $B_t = -0.6T$  and a plasma current  $I_p \sim 760kA$ . Density control was achieved via a feedback system, and the South-South (SS) NBI was injected with 1.4 MW of power to ensure reliable CXRS measurements. However, this scenario exhibited poor repeatability due to the occurrence of Internal Reconnection Events (IREs) during the ramp-up phase, which introduced uncertainty in the discharge evolution. The second, more recent campaign used the ELM coil configuration #17, corresponding to a perturbation with a relative phase of  $\Delta\Phi = 225^\circ$

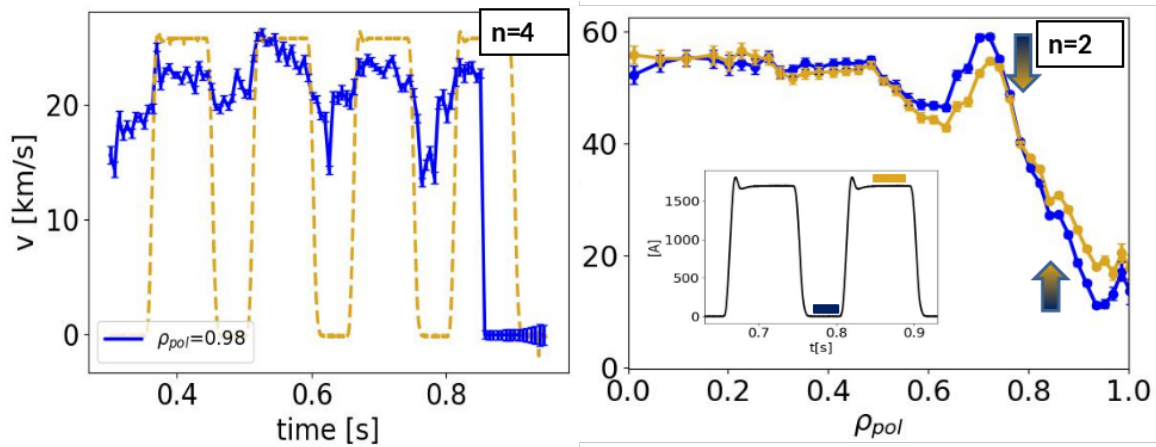


**Fig. 1** Left: edge time-trace of  $n = 4$  discharge (#50818). RMP waveform is overlaid. Right: Averaged toroidal velocity spatial profiles with (yellow) and without (blue) RMPs for one of the  $n = 2$  discharge (#51330). Here  $\rho$  is the square root of the normalized poloidal flux

between the upper and lower coil rows. A similar plasma scenario was employed, but with feed-forward density control during ramp-up, improving shot reproducibility and enabling systematic scans of RMP parameters. Throughout the discharges, electron density and temperature were measured with Thomson Scattering (TS), while ion temperature and toroidal velocity (based on carbon impurity rotation) were obtained via CXRS diagnostics. MHD activity was monitored using poloidal Mirnov probes and toroidal ex-vessel saddle coils. Notably, persistent but similar MHD activity was observed across the RMP parameter scans. In these experiments, the ELM coils were modulated in time to generate oscillatory magnetic perturbations. The rationale behind this choice has multiple reasons. For once, this approach allowed the assessment of the impact that varying modulation frequencies and amplitudes have on the equilibrium flow. In particular, shots from #51327 to #51330 featured scans in both amplitude and frequency (see label of Fig2). Moreover, time modulation also facilitated Fourier analysis of the velocity signals, enhancing the ability to correlate flow response with the RMP actuation.

### Data Analysis

Clear correlation between the CXRS-measured toroidal velocity and the ELM coil waveform was observed both in  $n = 2$  and  $n = 4$  configurations. Notably, near the separatrix, the toroidal velocity exhibited modulation synchronized with the RMPs, accelerating during their activation. The direction of acceleration was inferred from the temporal evolution at fixed radii and from comparative analysis of radial profiles with and without RMPs (see Fig1). A more quantitative assessment of this correlation was performed using a sinusoidal analysis. A key metric was the Signal-to-Noise Ratio (SNR) of the toroidal velocity's Fourier component at the ELM coil modulation frequency. In Fig2 SNR is shown versus the normalized radius ( $\rho$ ) for each discharge of the  $n = 2$  scan, defined as:  $SNR = v_{\phi}(f = f_{ELM})/v_{\phi}(f = f_{Noise})$ , where  $v_{\phi}(f)$  denotes the Fourier transform of the toroidal velocity signal. For square waveforms, only the frequency component with the highest amplitude was considered, simplifying the analysis and accounting for the typical suppression of higher harmonics. The noise level was computed as the average amplitude of the strongest components (excluding the signal frequency) within a  $\pm 10\text{Hz}$  window around  $f_{ELM}$ , excluding contributions below 2 Hz to filter global trends.

The analysis reveals several key trends. First, SNR increases with RMP amplitude, consistent with expectations. Second, at fixed amplitude, varying the modulation frequency alone does not yield significant changes in correlation strength. Third, in all discharges, SNR exceeds unity near the edge, supporting the presence of a robust correlation in the edge plasma. Interestingly, in discharge #51330, SNR also peaks at mid-radius. This can be explained by looking again at Fig 1 (left panel) in which evidences of a core-braking is observed when ELM coils are on. This suggests that the two peaks of the red curve of Fig 2 may originate from different physical mechanisms. Notably, discharge #51330 differs from the others in both waveform shape and maximum RMP amplitude, therefore further experiments are required to determine whether this behavior reflects a threshold effect or changes in RMP penetration dynamics.

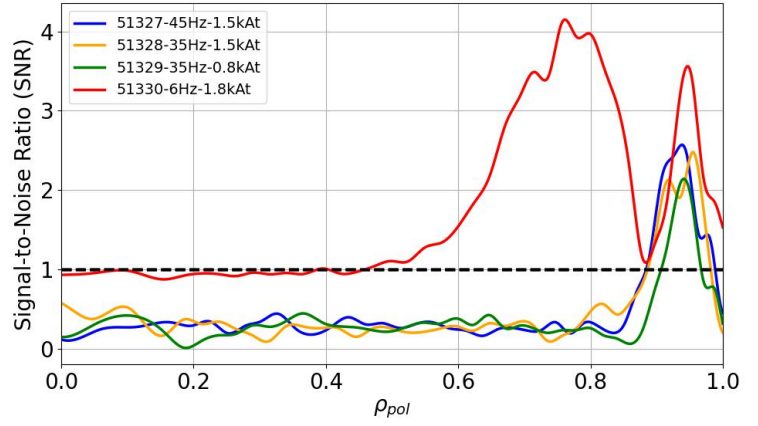
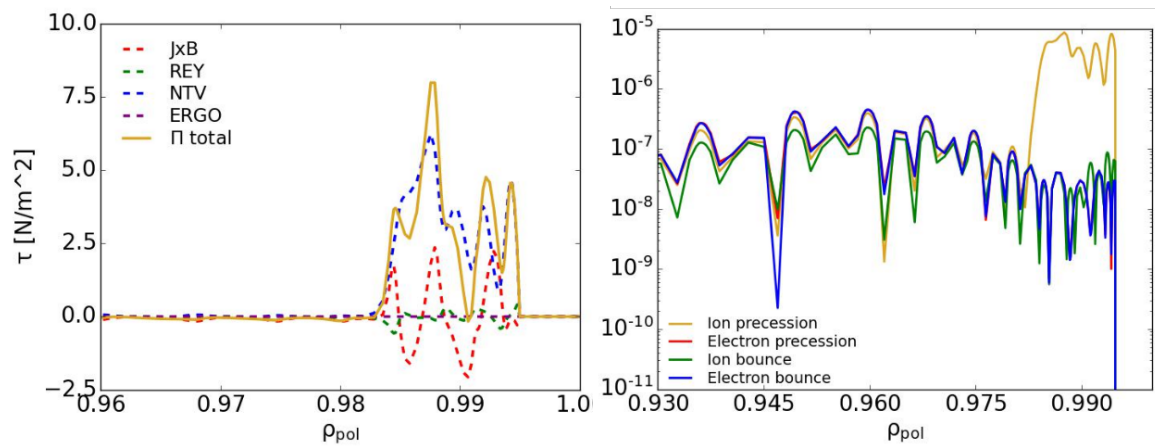


Fig. 2 FFT analysis of the  $n = 2$  scan

### Modeling

A numerical effort was undertaken with two primary objectives: (1) to reproduce and potentially explain the observed edge acceleration, and (2) to numerically characterize the RMP-induced torque. This was accomplished using the CHEASE/MARS-K workflow. CHEASE[7] is a well-established Grad-Shafranov equilibrium solver, while MARS-K[8] is a linear, single-fluid, visco-resistive MHD code capable of incorporating drift-kinetic corrections for various particle species to compute the plasma response to external magnetic perturbations. The workflow requires equilibrium data and kinetic profiles, along with applied perturbations. The former were obtained from the least perturbed discharge (#51329) at a stationary time slice, when RMPs were off, with kinetic profiles fitted using kineticEFIT to ensure consistency with measurements. The perturbation input, on the other hand, was constructed based on the coil currents from the most perturbed discharge (#51330). The exact coil geometry in configuration #17 was modeled using the ERGOS[9] code, which outputs the vacuum field associated with the applied RMPs. This vacuum field was then mapped to the MARS-K computational grid using the Equivalent Surface Current (ESC) technique. MARS-K was subsequently used to compute the plasma response and to estimate the RMP-induced toroidal torques. The code internally calculates both the MHD torques (including electromagnetic  $J \times B$  and Reynolds stress contributions) and the NTV torque, the latter derived from the identity  $\tau_{NTV} = -2 * Im(\delta W_K)$ [10], where  $\delta W_K$  denotes the perturbed kinetic energy tensor. Recently, the computation of the torque generated by the field line stochasticization has also been implemented following the theory proposed in [2]. Most notably, MARS-K predicts a positive total torque density localized in the outer region ( $\rho > 0.98$ ). Analysis of the torque components indicates that this positive edge torque is predominantly due to NTV, which is only partially counteracted by the electromagnetic braking from the  $J \times B$  term. This finding motivated a more detailed investigation of the NTV torque. In general, NTV becomes significant when one or



**Fig. 3** *Left* Total torque densities and all the components in the edge region as modeled by MARS-K. *Right* NTV torque density (in log-space), in the edge region, computed for each single resonance

more resonant conditions are satisfied. In the current implementation, only thermal ion and electron species were considered, which is justified given that any torque contribution from the supra-thermal NBI population would primarily affect the core. Quite surprisingly, the dominant contribution arises from the ion precession drift resonance. Although this is frequently the case in literature, standard NTV theory predicts that this resonance should always exert a counter- $I_p$  torque [11][5]. However, this seems now in discrepancy with current MARS-K results.

### Conclusions and Outlooks

In this study direct experimental evidence of an edge toroidal acceleration obtained in response to externally applied RMPs in MAST-U has been highlighted. Both  $n = 2$  and  $n = 4$  configurations induced clear changes in rotation, strongly correlated with the RMP coil waveform. Modeling suggests that the dominant torque originates from NTV effects at the plasma edge, with weaker stochastic contributions and braking MHD torques in the core. Future efforts will focus on expanding the analysis to potential density modulation using Doppler BackScattering (DBS), as well as applying gyrokinetic modeling with the GENE code to quantify the experimentally observed torque and to directly compare with modeling results. Comparative experiments in H-mode plasmas and devices with different aspect ratios and different heating sources to better characterize this RMP induced acceleration, are foreseen.

This work has been carried out within the framework of the EUROfusion Consortium, funded by the European Union via the Euratom Research and Training Programme (Grant Agreement No 101052200 — EUROfusion). Views and opinions expressed are however those of the author(s) only and do not necessarily reflect those of the European Union or the European Commission. Neither the European Union nor the European Commission can be held responsible for them.

### References

- [1] K. H. Finken et al. In: *Contributions to Plasma Physics* 46 (7-9 2006).
- [2] E. Kaveeva, V. Rozhansky, and M. Tendler. In: *Nuclear Fusion* 48 (7 2008).
- [3] A. M. Garofalo et al. In: *Physics of Plasmas* 16 (5 2009).
- [4] H. Sheng et al. In: *Physics of Plasmas* 31 (3 2024).
- [5] Y. Sun et al. In: *Nuclear Fusion* 51 (5 2011).
- [6] Y. Liu et al. In: *Nuclear Fusion* (2020).
- [7] H. Lütjens, A. Bondeson, and O. Sauter. In: *Computer Physics Communications* 97 (1996).
- [8] Y. Liu et al. In: *Physics of Plasmas* 15 (11 2008).
- [9] M. Bécoulet et al. In: *Nuclear Fusion* 48 (2 2008).
- [10] J. K. Park. In: *Physics of Plasmas* 18 (11 2011).
- [11] Y. Sun et al. In: *Nuclear Fusion* 53 (9 2013).